RESIDUAL STRESSES RESULTING FROM GROWTH AND REMODELING IN ARTERIAL WALLS

DANIEL BALZANI[†*] AND ANNA ZAHN[†]

[†]Institute of Mechanics and Shell Structures, Department of Civil Engineering
Technische Universität Dresden
01062 Dresden, Germany
Web page: https://imf.tu-dresden.de

[*]Dresden Center for Computational Materials Science (DCMS)
01062 Dresden, Germany
e-mail: daniel.balzani@tu-dresden.de

Key words: Biomechanics, Multiplicative Growth, Fiber Remodeling, Residual Stresses

Abstract. A model for multiplicative anisotropic growth in soft biological tissues, which relates the growth tensor to the fibrous tissue structure, is combined with a fiber remodeling framework. Both adaptation mechanisms are supposed to be governed by the intensity and the directions of the tensile principal stresses. Numerical examples on idealized arterial segments, illustrating stress and fiber angle distributions as well as resulting residual stresses in cases with and without fiber remodeling, are presented. It turns out that all processes including growth and remodeling are necessary to obtain qualitatively realistic distributions of fiber orientations, residual stresses, and stresses under loading.

1 INTRODUCTION

Being exposed to changes in its mechanobiological environment, arterial tissue continously strives to optimize its load-bearing capacities by adapting to altering conditions, for example to a sustained elevation of the blood pressure. This optimization procedure is characterized by growth and remodeling processes and is supposed to be the source of residual stresses which are typically existent in externally load-free states. Since these residual stresses are held responsible to reduce stress magnitudes and gradients in loaded states, they have to be accounted for in numerical simulations, see e. g. [4, 14, 18]. Constitutive equations for soft biological tissues commonly describe the anisotropic material behavior by modeling the tissue as an isotropic matrix material with embedded fibers. Based thereon, the reorientation of fibers and the addition of supplementary material can be considered to model adaptation processes and to quantify the associated residual

stresses. For both mechanisms, the intensity and the direction of principal stresses are assumed to be of particular importance.

Starting with the modeling of growth processes, an anisotropic growth model based on the multiplicative decomposition of the deformation gradient into a growth tensor and a remaining elastic part [15] is presented. In existing approaches based on this decomposition, e.g. in [8, 16], structural directions are used to incorporate growth in specific directions, for instance the radial direction in an artery. Here, a general local formulation is proposed, where the growth tensor is related to the fibrous tissue structure, which again is supposed to be directly linked to the directions of the highest (tensile) principal stresses. Establishing such a relation between the orientation of the fibers and the growth directions, the consequential extension of the model is to take remodeling of the fibers into account. A reorientation of the fibers ending up in a realistic arrangement, as for example discussed in [9, 7], is then expected to have twofold effects: an advantageous redistribution of the stresses and a direct influence on the growth directions, which are automatically adapted such that a reduction of high principal stresses is promoted. The basic assumption motivating both aspects of the combined framework is a symmetric alignment of the two fiber families in arteries with respect to the tensile principal stresses, which are supposed to be mainly located in the plane of the vessel wall. Following this assumption, a growth tensor designed to reduce the tensile principal stresses and an algorithm for the rearrangement of the fibers is proposed here.

2   BASICS OF THE COMPUTATIONAL MODEL

2.1   Growth model

A multiplicative decomposition of the deformation gradient $\boldsymbol{F} = \boldsymbol{F}_{\mathrm{e}}\boldsymbol{F}_{\mathrm{g}}$ is one of two methods frequently adopted to describe growth in soft biological tissues [1, 6]. The growth deformation arising from the growth part $\boldsymbol{F}_{\mathrm{g}}$ is characterized by a stress-free volume change increasing the reference volume with a factor $J_{\mathrm{g}} = \det[\boldsymbol{F}_{\mathrm{g}}]$. The second part of the deformation gradient, the elastic part $\boldsymbol{F}_{\mathrm{e}} = \boldsymbol{F}\boldsymbol{F}_{\mathrm{g}}^{-1}$ is linked with the deformation from the intermediate, grown state to the actual configuration, which is accompanied by the emergence of stresses. A polyconvex hyperelastic formulation for fiber-reinforced soft biological tissues of Balzani et al. [3] is applied, where the stresses are computed by differentiating a polyconvex strain energy function with respect to the deformation tensor. The 2$^{\mathrm{nd}}$ Piola-Kirchhoff stress tensor in the intermediate configuration is obtained by $\boldsymbol{S}_{\mathrm{e}} = 2\,\partial\psi/\partial\boldsymbol{C}_{\mathrm{e}}$ with the elastic part of the deformation tensor $\boldsymbol{C}_{\mathrm{e}} = \boldsymbol{F}_{\mathrm{g}}^{-T}\boldsymbol{C}\boldsymbol{F}_{\mathrm{g}}^{-1}$. The growth tensor $\boldsymbol{F}_{\mathrm{g}}$ can not be determined from equilibrium conditions [1] and thus has to be postulated by means of assumptions regarding growth directions and evolution equations. In the simplest case of isotropic growth with $\boldsymbol{F}_{\mathrm{g}} = \vartheta\boldsymbol{I}$ for instance, a single growth factor ϑ is involved. Based on an evolution equation $\dot{\vartheta} = k_{\vartheta}(\vartheta)\,\phi(\boldsymbol{Z})$, which is formulated in terms of the growth-driving quantity $\phi(\boldsymbol{Z})$, and the growth function k_{ϑ}, which includes time-dependency and prevents unlimited growth, the growth factor ϑ can

be identified [11]. Due to their material composition including a multitude of fiber-reinforced layers, the material behavior of soft biological tissues is highly non-linear and anisotropic. From the mechanical point of view, the complex tissue structure can be idealized by an isotropic ground matrix with embedded fibers, which are mainly arranged in two directions. Based on this idealization, the stress-strain-relation of soft biological tissues can be approximated by constitutive equations. Adaptation processes aim at reducing strains or stresses or their gradients within the loaded tissue state, which are thus governed by the microstructure, i.e. by the fiber reinforcement. It is therefore reasonable to assume that the tissue composition plays an important role in the context of adaptation processes as well, which leads to the conclusion that purely isotropic growth as mentioned above may not be sufficient.

Focusing on the reduction of principal stresses, an increase of the cross-section perpendicular to the direction of the principal stress appears reasonable. Such a growth process can be described by a growth tensor $\boldsymbol{F}_{\mathrm{g}} = \vartheta \boldsymbol{I} + (1 - \vartheta)\, \boldsymbol{A} \otimes \boldsymbol{A}$, where $\boldsymbol{A}$ is the direction of the principal stress. Arteries are thick-walled and tube-like structures which transform the internal pressure to tensile loads in the circumferential/axial plane of the wall. This is the reason why in arteries mainly two collagen fiber families are found within this plane. The particular orientation adapts to the stress state such that an improved load-bearing behavior is obtained. It is assumed that the orientations of the two fiber families are therefore defined symmetrically to the directions of the two highest principal stresses. With these two positive principal stresses (denoted by index I and II) which are sought to be reduced by growth, there are two directions which have to be taken into account for an appropriate definition of the growth tensor. To realize this, the growth tensor is multiplicatively decomposed into two parts $\boldsymbol{F}_{\mathrm{g}} = \boldsymbol{F}_{\mathrm{g}}^{(\mathrm{II})} \boldsymbol{F}_{\mathrm{g}}^{(\mathrm{I})}$ related to the first and second principal stress directions $\boldsymbol{A}_{\mathrm{g}}^{(\mathrm{I})}$ and $\boldsymbol{A}_{\mathrm{g}}^{(\mathrm{II})}$, where each part is defined as

$$\boldsymbol{F}_{\mathrm{g}}^{(a)} = \vartheta^{(a)} \boldsymbol{I} + \left(1 - \vartheta^{(a)}\right) \boldsymbol{A}_{\mathrm{g}}^{(a)} \otimes \boldsymbol{A}_{\mathrm{g}}^{(a)} \qquad \text{with} \qquad a = \mathrm{I}, \mathrm{II}. \tag{1}$$

The simple case of isotropic growth can casually be enclosed in the framework by setting the multiplicative parts of the growth tensor to $\boldsymbol{F}_{\mathrm{g}}^{(a)} = \vartheta^{(a)} \boldsymbol{I}$ with $a = \mathrm{I}, \mathrm{II}$, which allows a comparison of both approachs. Due to the split of the growth tensor into two parts, two independent growth factors $\vartheta^{(\mathrm{I})}$ and $\vartheta^{(\mathrm{II})}$ have to be derived from the two evolution equations

$$\dot{\vartheta}^{(a)} = k_{\vartheta}(\vartheta^{(a)})\, \phi^{(a)}(\boldsymbol{Z}^{(a)}), \qquad a = \mathrm{I}, \mathrm{II}. \tag{2}$$

The growth function k_{ϑ} is identically adopted from [12] for both growth factors. The growth-driving quantities $\phi^{(a)}$ are chosen such that those stress components are included, which are intended to be reduced, i.e. the principal stresses in the direction of the vectors $\boldsymbol{A}_{\mathrm{g}}^{(a)}$. Based on the isotropic driving force $\phi(\boldsymbol{C}_{\mathrm{e}} \boldsymbol{S}_{\mathrm{e}}) = \boldsymbol{C}_{\mathrm{e}} \boldsymbol{S}_{\mathrm{e}} : \boldsymbol{I}$ proposed in e.g. [11, 8, 16], the projections

$$\phi^{(a)}(\boldsymbol{C}_{\mathrm{e}} \boldsymbol{S}_{\mathrm{e}}) = \boldsymbol{C}_{\mathrm{e}} \boldsymbol{S}_{\mathrm{e}} : \boldsymbol{M}_{\mathrm{e}}^{(a)} \qquad \text{with} \qquad \boldsymbol{M}_{\mathrm{e}}^{(a)} = \boldsymbol{A}_{\mathrm{g}}^{(a)} \otimes \boldsymbol{A}_{\mathrm{g}}^{(a)}, \quad a = \mathrm{I}, \mathrm{II} \tag{3}$$

of the elastic part of the Mandel stress into the directions of the vectors $\boldsymbol{A}_{\mathrm{g}}^{(a)}$ are presumed in the context of anisotropic growth with the multiplicative parts of the growth tensor given by eq. (1). In case of isotropic growth, the isotropic measure $\phi^{(a)}(\boldsymbol{C}_{\mathrm{e}}\boldsymbol{S}_{\mathrm{e}}) = \boldsymbol{C}_{\mathrm{e}}\boldsymbol{S}_{\mathrm{e}} : \boldsymbol{I}$ ($a = \mathrm{I, II}$) is used. In both cases, each evolution equation depends on both growth factors $\vartheta^{(\mathrm{I})}$ and $\vartheta^{(\mathrm{II})}$ because strain and stress quantities in the intermediate configuration are involved which depend on the overall growth tensor $\boldsymbol{F}_{\mathrm{g}}$. For the numerical treatment of this coupled set of evolution equations see [21], where the procedure of computing the growth factors is described for the case of anisotropic growth. Once the growth factors $\vartheta^{(a)}$ have been identified, strains $\boldsymbol{C}_{\mathrm{e}}$ and stresses $\boldsymbol{S}_{\mathrm{e}}$ are known and the 2$^{\mathrm{nd}}$ Piola-Kirchhoff stress tensor $\boldsymbol{S} = \boldsymbol{F}_{\mathrm{g}}^{-1}\boldsymbol{S}_{\mathrm{e}}\boldsymbol{F}_{\mathrm{g}}^{-T}$ can be computed. Here, the tangent moduli $\mathbb{C} = 2\partial\boldsymbol{S}/\partial\boldsymbol{C}$ are computed numerically using a complex-step derivative approximation scheme [19]. Note that alternatively such schemes can also be applied to the implementation of the global tangent stiffness matrix [2].

2.2 Fiber remodeling

As another important mechanism in arterial tissue besides growth, fiber remodeling is part of the adaptation processes which optimize the load-bearing behavior. The combination of growth and fiber remodeling thus might result in stress distributions which are still more advantageous for the tissue.

In previous numerical examples, as e.g. in [21], the angles $\beta^{(1)}$ and $\beta^{(2)}$ between the fiber vectors and the direction of the first principal stress have been defined as constant over the wall thickness. This is however unrealistic since experimental observations show that the fiber angle is rather distributed through the thickness in healthy arteries. For atherosclerotic arteries, where a complex geometry of the artery is present and the idealization as a cylindrical tube is not applicable anymore, it becomes even more complex. Then, the circumferential, axial and radial directions, and thus the plane in which the fiber families are situated, are difficult to be defined. Therefore, an automated procedure to calculate realistic fiber directions is required, in particular for patient-specific analysis. For the calculation of the fiber orientation vectors subjected to stress-driven remodeling, the definition of the plane of the fiber families as the plane of the first two principal stresses is not sufficient, since it does not allow the determination of the orientation within the plane and thus, the fiber angles $\beta^{(a)}$. Therefore, an additional hypothesis postulated by Hariton et al. [9] is accounted for. Their fiber remodeling mechanism is based on the assumption that the fiber angles with respect to the principal directions are regulated by the ratio of the tensile principal stresses. Then, the target orientation of the fiber vectors in the actual configuration can be expressed by

$$\boldsymbol{a}_{\mathrm{targ}}^{(1)} = \langle\sigma_{\mathrm{I}}\rangle\,\boldsymbol{e}_{\mathrm{I}} + \langle\sigma_{\mathrm{II}}\rangle\,\boldsymbol{e}_{\mathrm{II}} \qquad \text{and} \qquad \boldsymbol{a}_{\mathrm{targ}}^{(2)} = \langle\sigma_{\mathrm{I}}\rangle\,\boldsymbol{e}_{\mathrm{I}} - \langle\sigma_{\mathrm{II}}\rangle\,\boldsymbol{e}_{\mathrm{II}}, \qquad (4)$$

where $\boldsymbol{e}_{\mathrm{I}}$ and $\boldsymbol{e}_{\mathrm{II}}$ are unit vectors in the directions associated with the first and second principal stresses σ_{I} and σ_{II}. These are in turn determined by solving the characteristic equation $\det[\boldsymbol{\sigma} - \sigma\boldsymbol{I}] = 0$ of the eigenvalue problem. The use of the Macaulay brackets

$\langle \bullet \rangle = \frac{1}{2}(|| \bullet || + \bullet)$ guarantees that only positive principal stresses are taken into account. It hence embeds the case of only one tensile principal stress, which may occur in arteries growing strongly in axial direction. Then, both fiber families will arrange in circumferential direction, cf. the numerical examples. The formulation of the constitutive equations often requires knowledge of normalized fiber orientation vectors in the reference configuration, which are given by

$$\boldsymbol{A}_{\text{targ}}^{(a)} = \frac{\boldsymbol{F}^{-1}\boldsymbol{a}_{\text{targ}}^{(a)}}{||\boldsymbol{F}^{-1}\boldsymbol{a}_{\text{targ}}^{(a)}||} , \qquad a = 1, 2. \tag{5}$$

The algorithmic treatment of the fiber remodeling model within the framework of finite elements is implemented as proposed by Fausten et al. [7]. There, at first an initial boundary value problem is solved where the external loads and an initial fiber orientation is prescribed. Then, the target fiber vectors are computed based on the assumptions given above. Setting the fiber orientations to the target orientations will influence the stress and strain distribution and thus, again equilibrium has to be accomodated by solving for the resulting displacements. In the context of a nonlinear Finite Element implementation this means that for large changes in the fiber orientation vectors the initial values for the Newton iterations will not be suitable. For this reason, the fiber orientation vectors are updated incrementally, applying only fractions of the whole difference vectors $\boldsymbol{A}_{\text{targ},0}^{(a)} - \boldsymbol{A}^{(a)}$ in such a way, that the change in the fiber angle does not exceed a predefined value. Further details concerning the fiber remodeling approach can be found in [7].

2.3 Combined approach

The presented framework for anisotropic growth in arterial walls relies on the assumption that growth can effectively reduce stresses if it occurs in the planes whose normal vectors are the directions $\boldsymbol{e}_{\text{I}}$ and $\boldsymbol{e}_{\text{II}}$ of the tensile principal stresses. Combining the growth model with the fiber remodeling framework, it is ensured that the two included families of collagen fibers are always arranged symmetrically with respect to the principal stress directions. This allows an identification of the principal stress directions from the fiber orientations, i. e.

$$\boldsymbol{e}_{\text{I}} = \frac{\boldsymbol{A}^{(1)} + \boldsymbol{A}^{(2)}}{||\boldsymbol{A}^{(1)} + \boldsymbol{A}^{(2)}||} \qquad \text{and} \qquad \boldsymbol{e}_{\text{II}} = \frac{\boldsymbol{A}^{(1)} - \boldsymbol{A}^{(2)}}{||\boldsymbol{A}^{(1)} - \boldsymbol{A}^{(2)}||} . \tag{6}$$

The vectors $\boldsymbol{A}_{\text{g}}^{(a)}$ in eq. (1) are then trivially given by

$$\boldsymbol{A}_{\text{g}}^{(\text{I})} = \boldsymbol{e}_{\text{I}} \qquad \text{and} \qquad \boldsymbol{A}_{\text{g}}^{(\text{II})} = \boldsymbol{e}_{\text{II}}. \tag{7}$$

With this relations at hand, it is possible to define an anisotropic growth tensor based on the local tissue microstructure, and there is no need of computing structural, geometric directions like the radial, circumferential or axial direction which do in general not coincide with the global coordinate system in patient-specific geometries. In this contribution we

propose to include a growth evolution as soon as the boundary value problem changes, i. e. not only if time proceeds or the loading conditions change, but also if a new fiber orientation is computed. However, we are rather interested in the final saturated state of fiber orientation and stress distribution than in the time-evolution of this process and thus, the growth velocities can be set rather arbitrarily. They will however, influence to some extent the results since faster/slower growth would change the stresses within each remodeling step. Therefore, these velocities can be considered as parameters to the algorithm, which require further analysis. On the other hand, if one was interested in the evolution of growth and remodeling instead of the final saturated state the values of the growth velocities would rather be physical parameters.

2.4 Residual stresses

Residual stresses in arterial walls and the related deformations are three-dimensional and thus strongly dependent on the radial and on the axial position within the vessel. A single parameter is therefore not suitable to entirely characterize the residual stress state [10]. However, since the early attempts of quantifying the magnitude of residual stresses, see e. g. [20], the opening angle experiment is often picked up to explain and to visualize the existence of residual stresses in arterial segments. It is therefore desirable to provide the possibility of simulating such experiments numerically. In this context, axial and radial cuts through the arterial wall have to be simulated in order to permit the expected deformations, namely a contraction in axial direction and an opening of the segment to a certain degree referred to as opening angle. Obviously, such a sudden change of the boundary conditions of a residually stressed body is followed by large deformations which can not be computed in a single step within a non-linear Finite Element framework. Therefore, an alternative procedure, which enables a stepwise identification of the final deformed state, has to be applied. This procedure, see [21] for details, is based on the definition of a secondary boundary value problem using the grown and deformed geometry of the residually stressed arterial segment with altered boundary conditions. In absence of any external load, the stress tensor is updated internally in several steps, such that the related deformation steps are small enough.

It is worth mentioning that the proposed method is also applicable to compute layer-specific opening angles in multilayered arterial segments. The numerical examples in the following section are nonetheless restricted to idealized, one-layered arterial segments and focus on the effect of adding a fiber remodeling formulation to the preexistent growth model, which has also an effect on the residual stresses and deformations. The mentioned opening angle is defined to be the angle between one of the cut edges and the symmetry axis which divides the opened segment into two equal halves. Axial strain in the opened segments is computed with respect to the residually stressed geometry before applying the cuts. It is dependent on the radial position and therefore averaged over the wall thickness.

3 NUMERICAL EXAMPLES OF IDEALIZED ARTERIAL SEGMENTS

For the evaluation of the combined approach for growth and remodeling, idealized arterial segments with material and growth parameters according to Tab. 1 are loaded by an internal pressure of 16 kPa (120 mmHg) and by axial displacements of 8 % or 10 % of the initial length. Five different arterial segments are considered for each load case: a reference segment without growth and remodeling as well as an isotropically and an anisotropically growing segment, each of them with and without remodeling. The initial fiber orientation vectors of two reinforcing fiber families are defined such that they enclose $\pm 30°$ with the circumferential direction. Within the first second of the simulation time, the loads are simultaneously applied and afterwards held constant until $t = 20$ s. During the entire time period, depending on the considered case, growth is enabled and remodeling is performed in each time step.

An overview of the resulting stress distributions at $t = 20$ s is given in Fig. 1 (a) for isotropic and Fig. 1 (b) for anisotropic growth. The dashed lines refer to the non-adapting reference segments, whereas solid lines are used for the growing segments (luscious colors) and for the segments where growth and remodeling is taken into account (light colors). Several observations concerning remodeling can be noted. Remodeling strongly reduces

Table 1: Material parameters for arterial tissue [5] and (dimensionless) parameters of the function k_ϑ from [12] used in the numerical examples.

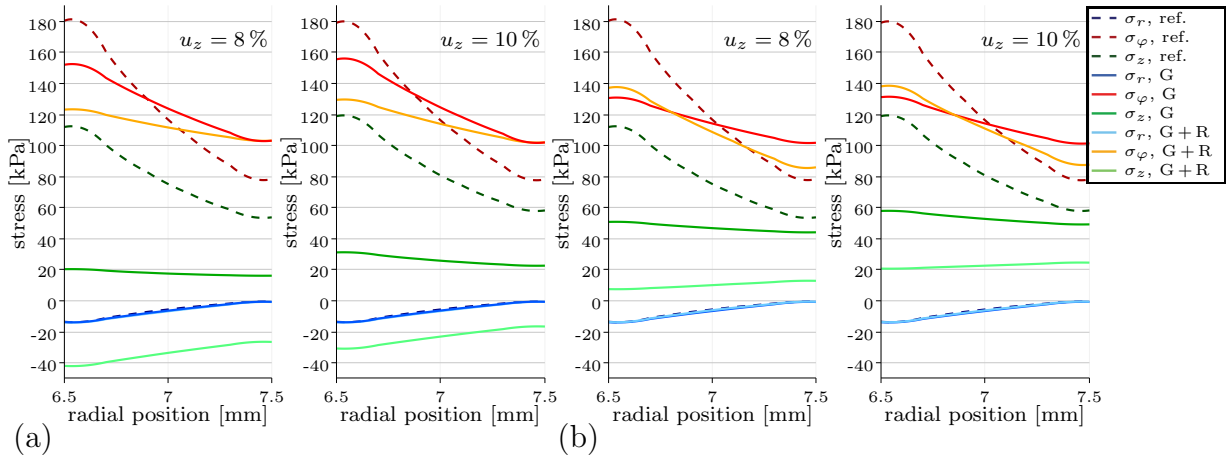| c_1 [kPa]	ϵ_1 [kPa]	ϵ_2 [-]	α_1 [kPa]	α_2 [-]	ϑ^+	k_ϑ^+	m_ϑ^+	ϑ^-	k_ϑ^-	m_ϑ^-
17.5	499.8	2.4	30 001.9	5.1	1.1	1.0	3.0	0.9	1.0	3.0

Figure 1: Radial, circumferential and axial stresses in the arterial segments at $t = 20$ s for (a) isotropic and (b) anisotropic growth with and without remodeling at different levels of axial displacement. In each diagram, the reference stresses of the non-growing and non-remodeling artery are given as dashed lines.
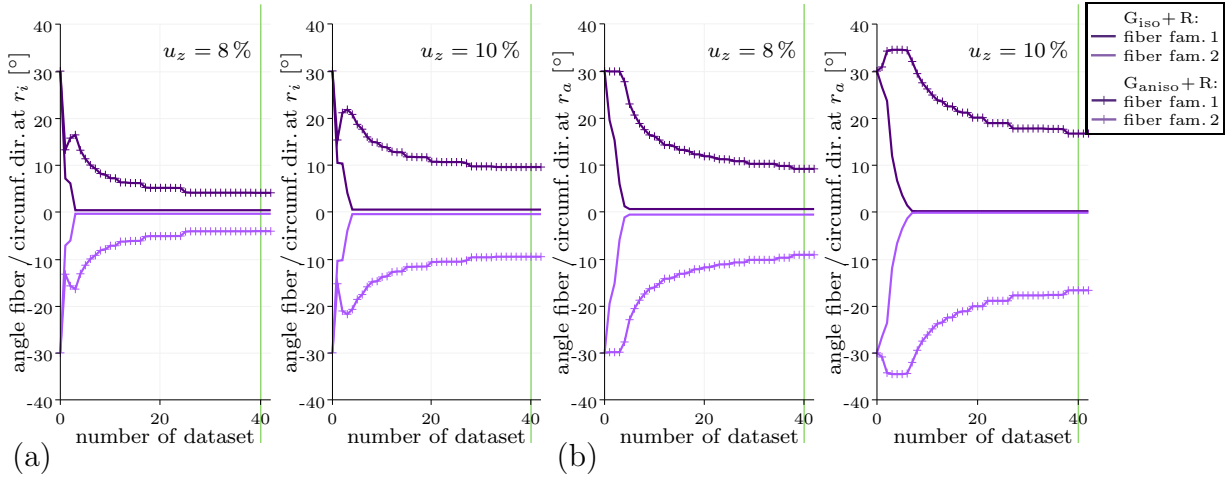
Figure 2: Development of the fiber orientation angles over time at (a) the inner surface and (b) the outer surface of the arterial segment for axial displacements of 8 % and 10 % and for isotropic (solid lines) and anisotropic growth (solid lines with markers). The number of dataset divided by 2 corresponds to time in s. At $t = 20$ s, remodeling is deactivated and no more change of the fiber angles takes place.

the axial stresses, especially if isotropic growth is active. This implies that the axial stresses, which are already strongly reduced by growth alone, may fall below zero and become compressive depending on the growth model and the value of the axial displacement. The impact of remodeling on the circumferential stresses varies from case to case. In combination with anisotropic growth, remodeling induces a slight increase of the circumferential stress peak and gradient, the differences between arterial segments with 8 % and 10 % axial displacement are marginal. In contrast to that, positive effects of remodeling on the circumferential stress distributions can be stated in combination with isotropic growth. The circumferential stress peaks are even lower than in the corresponding anisotropically growing segments without remodeling. Moreover, the dependence of the circumferential stresses on the axial displacement is more pronounced if isotropic instead of anisotropic growth is considered.

In Fig. 2 (a) and (b), the development of the angles over the remodeling process between the fiber orientation vectors and the circumferential direction at the inner and at the outer surface of the remodeling arterial segments is shown. Significant differences indicate that the remodeling results are fairly sensitive with respect to the chosen growth model and/or the height of the axial displacement. In isotropically growing segments, where the axial component of growth is larger than in anisotropically growing ones, compressive axial stresses result in an alignment of both fiber families in circumferential direction over the whole wall thickness. For the anisotropically growing segments, the level of axial strain is high enough to obtain two tensile principal stresses. Then, the fibers arrange with angles that are distributed over the wall thickness and lie between 4° and 9° or 9.5° and 16.5° for axial displacements of 8 % or 10 % at the end of the simulated time period, which is rather in line with experimental observations [13, 17].
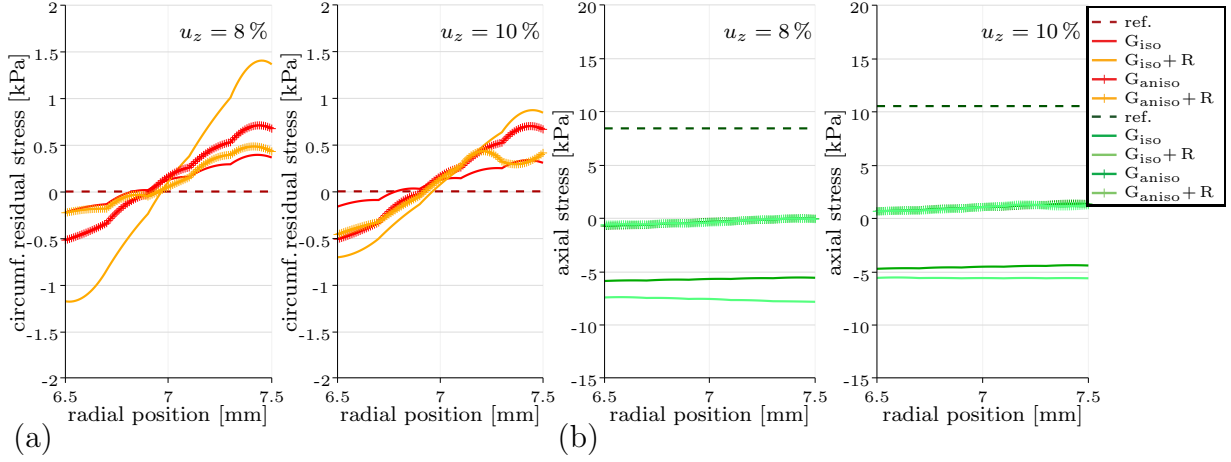
Figure 3: (a) Circumferential residual stresses and (b) axial stresses arterial segments subjected to isotropic or anisotropic growth with and without remodeling at $t = 20\,\mathrm{s}$ after removal of the internal pressure while retaining the axial displacement.

The effect of remodeling on the residual stresses is illustrated in Fig. 3, where the circumferential and the axial stress distributions after the removal of the internal pressure are given. The axial displacement is retained in order to be able to simulate radial and axial cuts in the segments afterwards. Therefore, the axial stresses in Fig. 3 (b) are no residual stresses in the classical meaning since axial loading is still present. Without remodeling, the circumferential residual stresses are almost independent on the two different axial displacements, which can also be seen at the corresponding opening angles given in Tab. 2. This changes drastically if remodeling is included. In combination with isotropic growth, remodeling increases residual stresses and opening angles. In contrast to that, the opposite happens in combination with anisotropic growth. For the considered axial displacements, axial stresses are influenced by remodeling only in case of isotropic growth. Contradicting experimental observations, most of the arterial segments extend after release of the axial boundary, see Tab. 2. However, this could be resolved by applying larger

Table 2: Opening angles and mean axial strain in (residually) stressed arterial segments after simulation of radial and axial cuts.

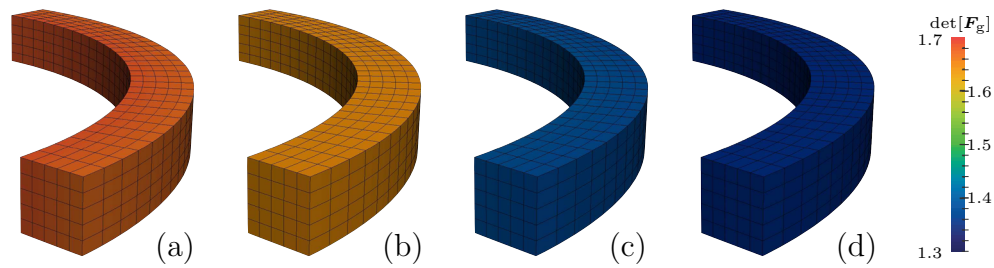| axial displacement	reference case	isotropic growth	isotropic growth + rem.	anisotropic growth	anisotropic growth + rem.
8 %	0.18°	6.94°	32.59°	11.54°	6.15°
10 %	0.45°	5.09°	21.28°	11.12°	8.68°
8 %	−7.8 %	5.5 %	7.3 %	0.5 %	0.5 %
10 %	−9.9 %	4.5 %	5.4 %	−0.9 %	−0.9 %

Figure 4: Comparison of the growth deformation of (a) isotropically growing, (b) isotropically growing and remodeling, (c) anisotropically growing and (d) anisotropically growing and remodeling arterial segments subjected to an internal pressure of $16\,\mathrm{kPa}$ and an axial displacement of $8\,\%$.

axial displacements which indicates that there may be rather large axial average loads in arteries. In Fig. 4, the determinant J_g of the growth tensor is illustrated to clarify the effect of remodeling on the growth deformation. Arterial segments with activated fiber remodeling manifest lower volume increases than the corresponding segments with fixed fiber orientation vectors. This also holds for axial displacements of $10\,\%$.

4   CONCLUSIONS

A combined approach for growth and remodeling was proposed. Besides the enclosed possibility of simulating isotropic growth, anisotropic growth relating the growth tensor to the local fiber orientation vectors is the main feature of the growth model. In this regard, an automated computation of reasonable fiber distributions is an important enhancement of the model, which has been designed based on the assumption that the two dominating fiber families in arterial tissue arrange symmetrically with respect to the directions of the local tensile principal stresses.

The effects of remodeling on the stress and fiber angle distributions in simulated growing arterial segments were dependent on the chosen growth model and on the ratio between radial and axial loadings. It can be stated that circumferential stress peaks and gradients were reduced for the considered examples of isotropic growth and slightly increased if growth is anisotropic. In each example, remodeling provoked a reduction of axial stresses. As apparent here and also in [21], circumferential residual stresses resulting from isotropic or anisotropic growth were comparatively insensitive with respect to the intensity of the axial displacement. If remodeling was included, the sensitivity of the circumferential residual stresses and opening angles with respect to the axial displacement increased, which was probably caused by the fiber angle distribution with its dependence on the ratio between pressure and axial loading. Summarizing, qualitatively reasonable distributions of residual stresses and fiber orientations were obtained for the anisotropic growth model. Furthermore, it appears that this model does require less growth to enable these stress-regularizing distributions. The knowledge of the obtained fiber orientation vectors was the only necessity for the definition of the anisotropic growth tensor, which

is therefore a local property of the material point and does not depend on external geometric parameters which are difficult to obtain for patient-specific diseased arteries. The effect of the parameters of the growth model, which have been set rather intuitively and identically for each variation of the simulations so far, should be analyzed.

5 ACKNOWLEDGEMENT

REFERENCES

[1] Ambrosi, D.; Ateshian, G. A.; Arruda, E. M.; Cowin, S. C.; Dumais, J.; Goriely, A.; Holzapfel, G. A.; Humphrey, J. D.; Kemkemer, R.; Kuhl, E.; Olberding, J. E.; Taber, L. A.; Garikipati, K. Perspectives on biological growth and remodeling. *J. Mech. Phys. Solids* (2011) **59**:863–883.

[2] Balzani, D.; Gandhi, A.; Tanaka, M.; Schröder, J. Numerical calculation of thermo-mechanical problems at large strains based on a robust approximation scheme for tangent stiffness matrices. *Comput. Mech.* (2015) **55**:861–871.

[3] Balzani, D.; Neff, P.; Schröder, J.; Holzapfel, G. A. A polyconvex framework for soft biological tissues. Adjustment to experimental data. *Int. J. Solids Struct.* (2006) **43**:6052–6070.

[4] Balzani, D.; Schröder, J.; Gross, D. Simulation of discontinuous damage incorporating residual stresses in circumferentially overstretched atherosclerotic arteries. *Acta Biomater.* (2006) **2**:609–618.

[5] Brands, D.; Klawonn, A.; Rheinbach, O.; Schröder, J. Modelling and convergence in arterial wall simulations using a parallel FETI solution strategy. *Comput. Methods Biomech. Biomed. Engin.* (2008) **11**:569–583.

[6] Cyron, C. J.; Humphrey, J. D. Growth and remodeling of load-bearing biological soft tissues. *Meccanica* (2017) **52**:645–664.

[7] Fausten, S.; Balzani, D.; Schröder, J. An algorithmic scheme for the automated calculation of fiber orientations in arterial walls. *Comput. Mech.* (2016). **58**:861–878.

[8] Göktepe, S.; Abilez, O. J.; Kuhl, E. A generic approach towards finite growth with examples of athlete's heart, cardiac dilation, and cardiac wall thickening. *J. Mech. Phys. Solids* (2010) **58**:1661–1680.

[9] Hariton, I.; deBotton, G.; Gasser, T. C.; Holzapfel, G. A. Stress-driven collagen fiber remodeling in arterial walls. *Biomech. Model. Mechan.* (2007) **6**:163–175.

[10] Holzapfel, G. A.; Sommer, G.; Auer, M.; Regitnig, P.; Ogden, R. W. Layer-Specific 3D Residual Deformations of Human Aortas with Non-Atherosclerotic Intimal Thickening. *Ann. Biomed. Eng.* (2007) **35**:530–545.

[11] Kuhl, E.; Maas, R.; Himpel, G.; Menzel, A. Computational modeling of arterial wall growth. Attempts towards patient-specific simulations based on computer tomography. *Biomech. Model. Mechan.* (2007) **6**:321–331.

[12] Lubarda, V. A.; Hoger, A. On the mechanics of solids with a growing mass. *Int. J. Solids Struct.* (2002) **39**:4627–4664.

[13] O'Connell, M.K.; Murthy, S.; Phan, S.; Xu, C.; Buchanan, J.; Spilker, R.; Dalman, R.L.; Zarins, C.K.; Denk, W.; Taylor, C.A. The three-dimensional micro- and nanostructure of the aortic medial lamellar unit measured using 3D confocal and electron microscopy imaging. *Matrix Biology* (2008) **27**:171–181.

[14] Pierce, D. M.; Fastl, T. E.; Rodriguez-Vila, B.; Verbrugghe, P.; Fourneau, I.; Maleux, G.; Herijgers, P.; Gomez, E. J.; Holzapfel, G. A. A method for incorporating three-dimensional residual stretches/stresses into patient-specific finite element simulations of arteries. *J. Mech. Behav. Biomed. Mater.* (2015) **47**:147–164.

[15] Rodriguez, E. K.; Hoger, A.; McCulloch, A. D. Stress-dependent finite growth in soft elastic tissues. *J. Biomech.* (1994) **27**:455–467.

[16] Sáez, P.; Peña, E.; Martínez, M. A.; Kuhl, E. Computational modeling of hypertensive growth in the human carotid artery. *Comput. Mech.* (2014) **53**:1183–1196.

[17] Schriefl, A.J.; Zeindlinger, G.; Pierce, D.M.; Regitnig, P.; Holzapfel, G.A. Determination of the layer-specific distributed collagen fibre orientations in human thoracic and abdominal aortas and common iliac arteries. *J. Roy. Soc. Interface* (2012) **9**, doi = 10.1098/rsif.2011.0727.

[18] Schröder, J.; Brinkhues, S. A novel scheme for the approximation of residual stresses in arterial walls. *Arch. Appl. Mech.* (2014) **84**:881–898.

[19] Tanaka, M.; Fujikawa, M.; Balzani, D.; Schröder, J. Robust numerical calculation of tangent moduli at finite strains based on complex-step derivative approximation and its application to localization analysis. *Comput. Methods Appl. Mech. Engrg.* (2014) **269**:454–470.

[20] Vaishnav, R. N.; Vossoughi, J. Residual stress and strain in aortic segments. *J. Biomech.* (1987), **20**:235–239.

[21] Zahn, A.; Balzani, D. Modeling of Anisotropic Growth and Residual Stresses in Arterial Walls. *Acta Polytechnica CTU Proceedings* (2017) **7**:85–90.